

# Free fall 2D+ simulation with starccm+V4

V. Moreau,

*CRS4, Centre for Advanced Studies, Research and Development in Sardinia*

July 16<sup>th</sup> 2010

Version 1.1

## Abstract

The aim of this note is to gather some information on the free surface simulations with starccm+V4 of a 2D+ free falling jet. Two transient simulations are performed aimed at stabilizing the stagnation level where a free falling jet re-connect to the mainstream. While the main objective failed, some useful information on the condensation/sharpening algorithm used is gained.

## Contents

Free fall 2D+ simulation with starccm+V4 .....	1
1 Introduction .....	1
2 Technical framework .....	2
3 Geometry and setting .....	2
4 Results visualization and comment .....	5
5 Conclusion.....	8
6 References .....	8

## 1 Introduction

In the framework of the EUROTRANS European project [ 1], a Myrrha-like Target has been foreseen for the XT-ADS<sup>1</sup>. This target presents several difficult features from the CFD point of view. Mainly, it is a two-fluid flow composed of liquid Lead Bismuth Eutectic (LBE) and an extremely rarefied gas which can be considered as an almost perfect vacuum.

In the reference design, because of material issues, local velocities should remain below 2.5 m/s, the nominal flow rate being 13 l/s. In this simulation we want to capture the free fall aspect of the Myrrha/XT-ADS target, but avoid the more difficult axial-symmetrical central recirculation treatment. A former 2D axial-symmetrical simulation, performed with StarCD (Version 4.08), for a geometry similar to the reference target one showed a highly unstable central recirculation zone. Moreover, it has not be possible to get a reasonably stable reattachment point where the free falling liquid should connect to the bulk fluid region. The central recirculation instability is thought to be highly reinforced by the axial-symmetrical simulation, allowing only axial-symmetrical solutions. The reattachment instability is not clearly understood but may be related to the very small section allowed for the light phase. Both instabilities are apparent also because we could essentially get rid of the numerical smearing of the interface. Two plots of the volume fraction are shown in Figure 1.

---

<sup>1</sup> XT-ADS: eXperimenTal Accelerator Driven System

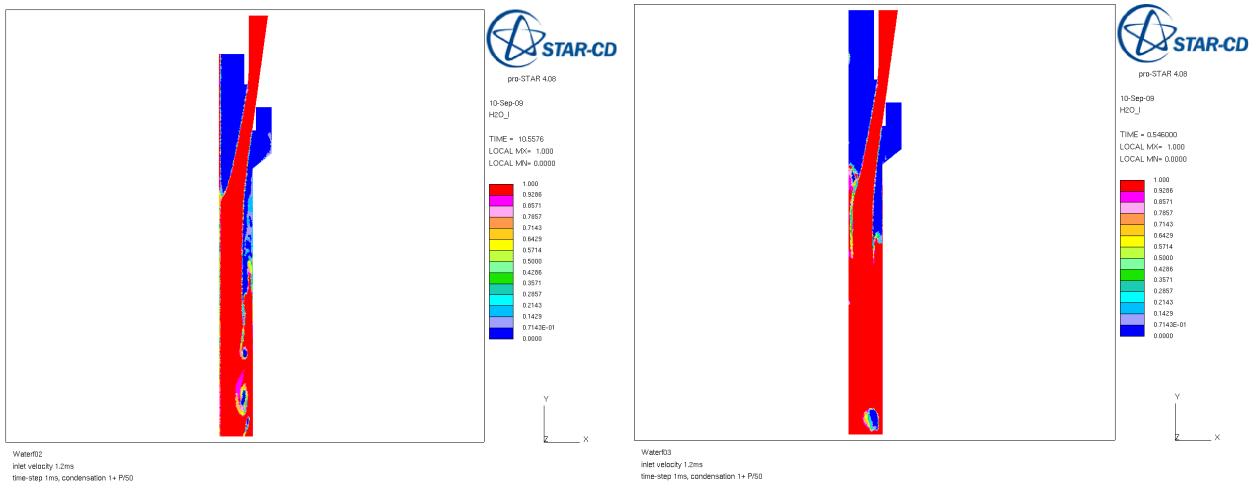


Figure 1: 2D axial-symmetrical slice of a XT-ADS spallation target. The simulation gave problems both at the symmetry axis and at the lower re-attachment level that could not be stabilized.

The simulation used a simple condensation/sharpening algorithm. By forcing condensation of the light phase on the heavy phase, we create a small wind towards the heavy phase that compensates for the traditional diffusive pattern common on former two-phase flows. The interface is thus kept sharp, but only by acting on the light phase. In this way, we can hope that the heavy phase flow is essentially left undisturbed.

The result is rather impressive and sharp interfaces are readily obtained, however without the usual rigidifying defect of convection scheme based sharpening algorithms.

By 2009, the number and variety of available physical models incorporated in Starccm+, and more specifically, the incorporation of the VOF model seemed sufficient to proceed to the change of reference CFD software.

We decided therefore that all further CFD investigations on free-surface flows will be performed with Starccm+. The first of these ones are presented hereafter.

## 2 Technical framework

The free surface simulations is performed with starccm+ versions 4.02 and successive. The geometry is elaborated using stardesign. It can be exported to starccm+ in parasolid format. Unfortunately, only relatively simple (block) geometries can be effectively exported. Otherwise, the mesh can be directly assembled in stardesign and, after initialization, the case can be saved in starccm+ format. From the version 4.06 of starccm+, stardesign is strongly linked to starccm+ and the transfer can be effectuated as soon as the geometry is built.

## 3 Geometry and setting

A previous test case was based on one of the axial-symmetrical designs of the XT-ADS water experiment. Performed on a 2D basis with triangular cells in StarcdV4, it has not be possible to stabilize the simulation, see Figure 1. The flow behaviour near the symmetry axis is heavily constrained by the imposed exact flow symmetry, leading to a degenerating configuration on the axis. Furthermore, the re-attachment level at which the falling fluid should connect with a more

stagnant zone could not be stabilized and showed a very chaotic behaviour. Nevertheless, the contraction algorithm showed to perform quite well.

The test case presented here is a relatively simple 2D+ free fall simulation. It is illustrated in Figure 2. By 2D+, we mean a simulation with a very small number of cells in the third dimension. Here we have about 3 cells, one central and one on both symmetry planes. Water is falling from a downward converging nozzle at about 2m/s and is let fall down freely for 30 up to 60 cm.

External total dimensions are: width 7 cm, height 80 cm, depth 2mm. The geometry is divided into five logical volumes:

1. The nozzle: top inlet width 5 cm, bottom outlet 2.5 cm, height 10 cm.
2. The top right gas exhaust: 2 cm wide and 10cm high.
3. The free fall volume: 40 cm high (30 cm high from nozzle bottom ), 7 cm wide.
4. The would be stagnant volume composed of a 20 cm high, 7 cm wide and a 5 cm high, 4 cm wide volume.
5. An exit volume, 5 cm high and 4 cm wide.

The volumes interfaces are shown on Figure 2 and on all volume fraction plots.

Motivation for this test case was to verify if we could get a relatively stable reattachment point with a slightly larger stagnation region and to evaluate the strength of the required interface sharpening algorithm. Also, the axial-stagnation region of the Myrrha target, which is believed to be the toughest affair there, is not contemplated here.

At first, we have tried to let the falling fluid impact the surface of a relatively stagnant fluid region. Control was performed by adjusting the outlet pressure and also by adjusting some porous resistance parameter at the interface between the stagnant and exit volumes. It has been found out that there seems to be no intermediary stable free surface level. The free surface either rising up to over the nozzle exit, or being transported back out of the computational domain. Both behaviour where obtained by just a slight variation in setting the outlet pressure.

A first transient simulation has been performed with the following parameters:

- Mesh size: 1.5 mm.
- Time step: 0.001s, switched to 0.0005s at time 32s.
- Top air pressure: 0.0 Pa (stagnation inlet)
- Inlet velocity: 1 m/s (nozzle outlet mean velocity 2 m/s)
- Air sink: 50 cd.
- Top porous baffle (base of air exhaust volume):  $(\alpha,\beta)=(2,0)$
- Bottom porous baffle: swiched from  $(\alpha,\beta)=(1,0.1)$  to  $(\alpha,\beta)=(1.2,0.1)$  after 4s.

After 2s of simulation, the air exhaust boundary condition was switched from pressure boundary, causing an inflow warning, to a stagnation inlet.

The control was effectuated by modifying the bottom outlet pressure value, according to the following table:

Time (s)	0-4	4-12	12-18	18-26	26-30	30-34
Bottom pressure (kPa)	0	1	3	2	1.5	1

Table 1: Outlet pressure evolution in time.

The first objective of this simulation was to stabilize a reasonable stationary solution with a reasonably fixed height of the bottom free surface level. Therefore a relatively large time step was used, together with a strong condensation. The condensation effect performed seemingly well, keeping the interface locally sufficiently sharp to be meaningful while the flow was perturbed by strong splashes. The volume fraction at different times is shown on Figure 3 and Figure 4. After 32s of simulation, we could consider to have fell the main objective. In effect, small outlet pressure variations seemed to induce large stagnation level variations, so that we did not manage to stabilize it around 30 cm below the nozzle exit, where the two larger logical volumes connect.

The water velocity at the nozzle exit is 2m/s. But the water accelerates quite a lot while free falling to reach about 4 m/s at the bottom of the numerical domain (see Figure 4, right). As the mesh size is 1.5 mm, with a time step of 0.001s the CFL is slightly above one at the nozzle exit, but increases quite a lot downstream. To evaluate the effect of the weak time resolution, the time step has been reduced to 5E-4s at time 32s, and the simulation has been run for two additional seconds. The result can be appreciated by comparing the last two volume fraction images in Figure 4. The fluid interface that was formerly slightly smeared while the flow was running downstream is completely re-contracted on a one cell width basis.

A second simulation, prosecution of the first one, has been performed, keeping the reduced time step or 5E-4s. This was a lousy attempt to reach a re-attachment quote 30 cm below the nozzle exits, hoping that the smaller time step and the better interface capture could make the flow less sensitive to the bottom pressure value.

The main variations of the second transient are reported in the table below.

Time (s)	3-5	5-12.2	12.2-16	16-20	20-28	28-31
Pressure (kPa)	2	2.5	2	2	1	0
( $\alpha, \beta$ )	1.2, 01			1.0, 0.1		1E-3, 1E-3

Table 2: Main variations of the second transient simulation.

After 28s, it has been decided to let the flow falling freely down to the simulation domain bottom exit. This was essentially completed after 1s at time 29s. After 29s, the light phase source term has been (almost) withdrawn, passing from -50 cd to -0.001 cd.

The volume fraction of water can be visualized at several times in Figure 5 and Figure 6.

The falling jet freely exiting through the bottom pressure boundary after 29s, we could test the usefulness of the condensation/sharpening algorithm. It resulted that the condensation was in this particular case completely useless (but not disturbing). By the way, the co-flow was organized in such a way that no strong shear flow would appear close to the falling fluid. The Eulerian sharpening convection algorithm performs therefore perfectly in absence of strong shear, for a controlled CFL order unity.

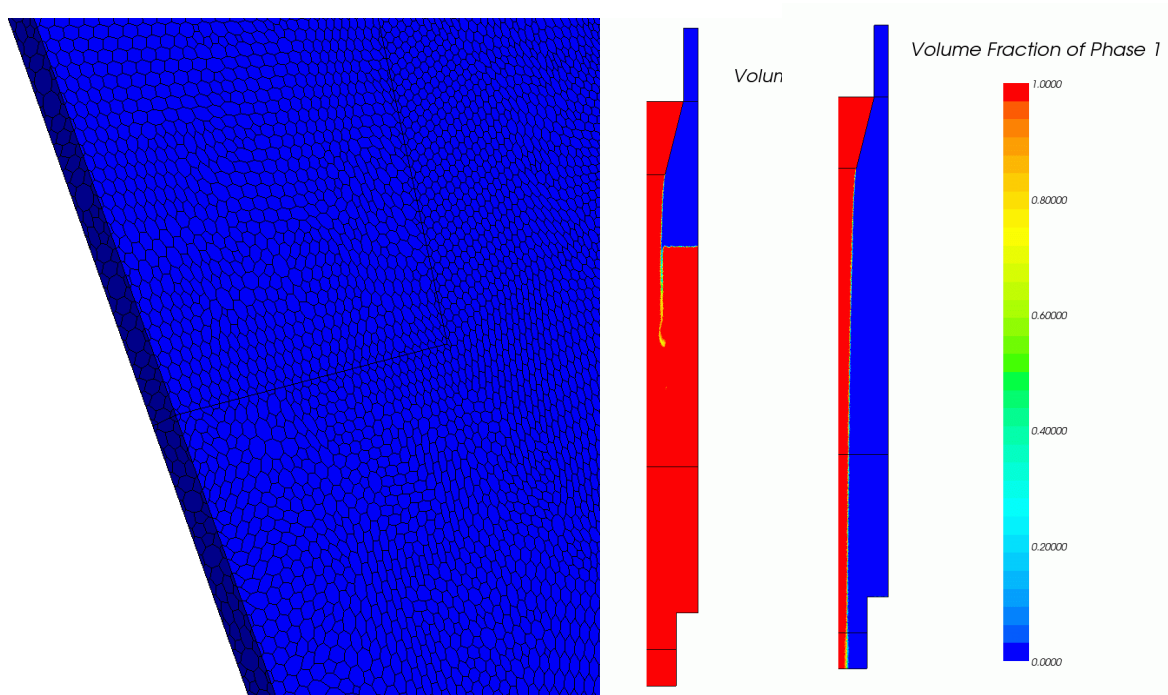


Figure 2: Free-fall test case. Left, a mesh detail. Centre and right: water volume fraction. Centre: free fall connects to a stagnation region. Right: free fall exits through the bottom pressure boundary.

Apart from the failure in getting a stagnation region at the desired level, these two simulations illustrate also some limitation of the 2D free surface flow. In effect, it is very unlikely that the time evolution of the entrained light phase at the intersection of the falling jet and the stagnation region would keep a 2D structure. We would more likely observe 3D structures like bubbles formations. Also, vortices that would keep a negative pressure in 2D are likely to be fed by flow coming from their extremities.

## 4 Results visualization and comment

The volume fraction of the two simulations is shown in the following figure for several simulation times.

The problem is that with a sharp interface, the simulation limitations related to the 2D approximation become critical. This can be made more clear once we observe that almost no change of the flow topology (bubble inclusion, droplet ejection, collapsing waves) is ever resolved in 2D in the real physical world. Moreover, only quasi stagnant free surface real flows are stationary, and the convenient interpretation of a diffuse interface as a temporal mean is no more allowable.

Managing to get a sharp interface, we are thus forced to renounce both to the 2D and to the stationary simulations, except for trivial useless free surface flows. Rephrasing positively, we must enter the world of 3D transient simulations.

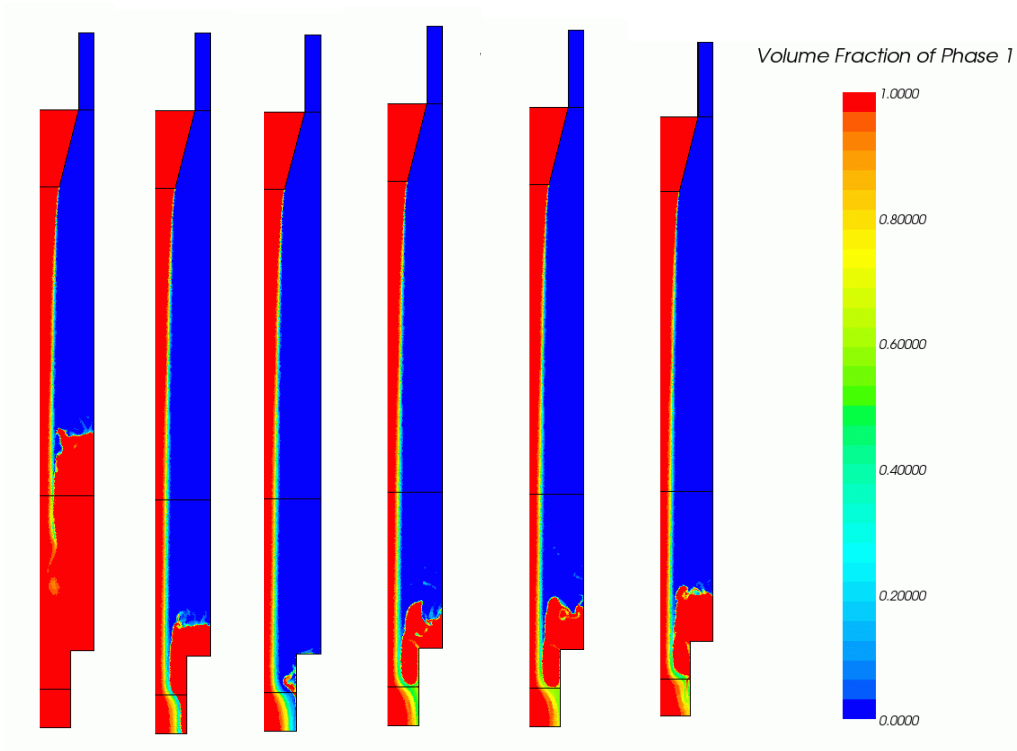


Figure 3: free fall first transient simulation. From left to right, volume fraction of water at times: 1s, 2s, 3s, 4s, 5s, 7s and 10s.

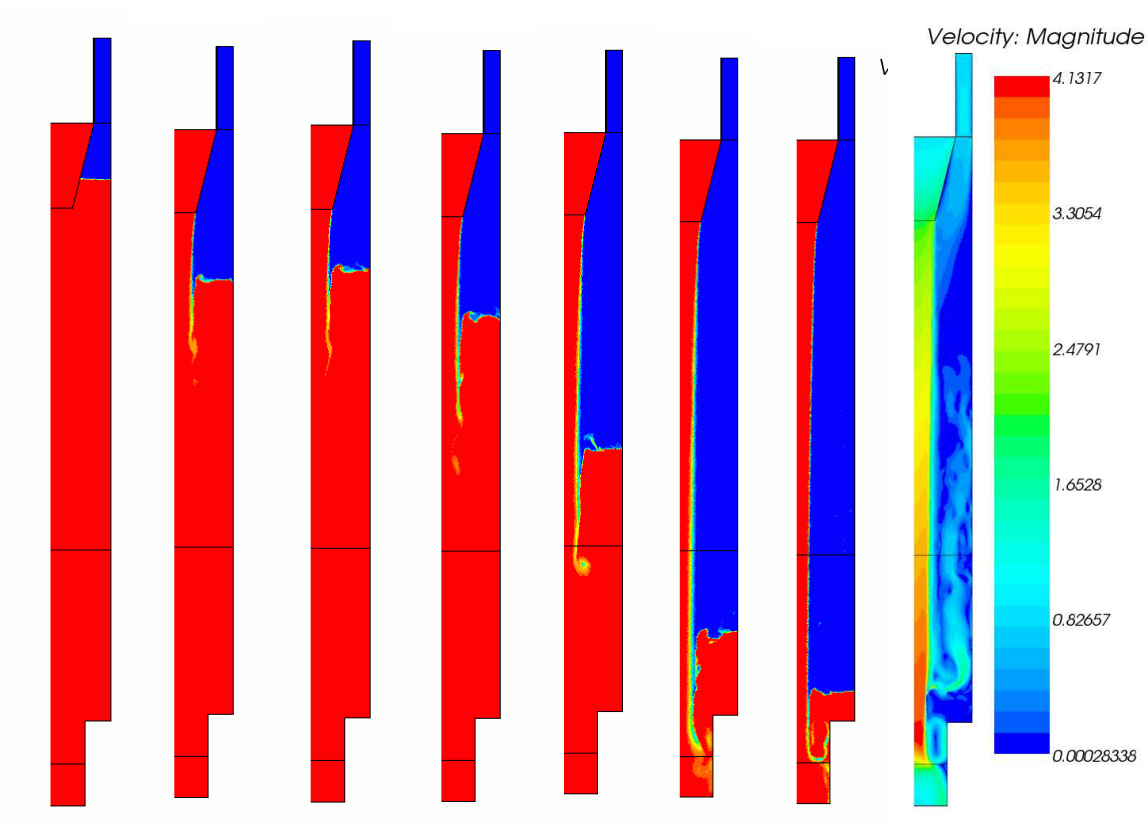


Figure 4: free fall first transient simulation. From left to right, volume fraction of water at times: 16s, 18s, 24s, 26s, 30s, 32s and 34s together with the velocity magnitude.

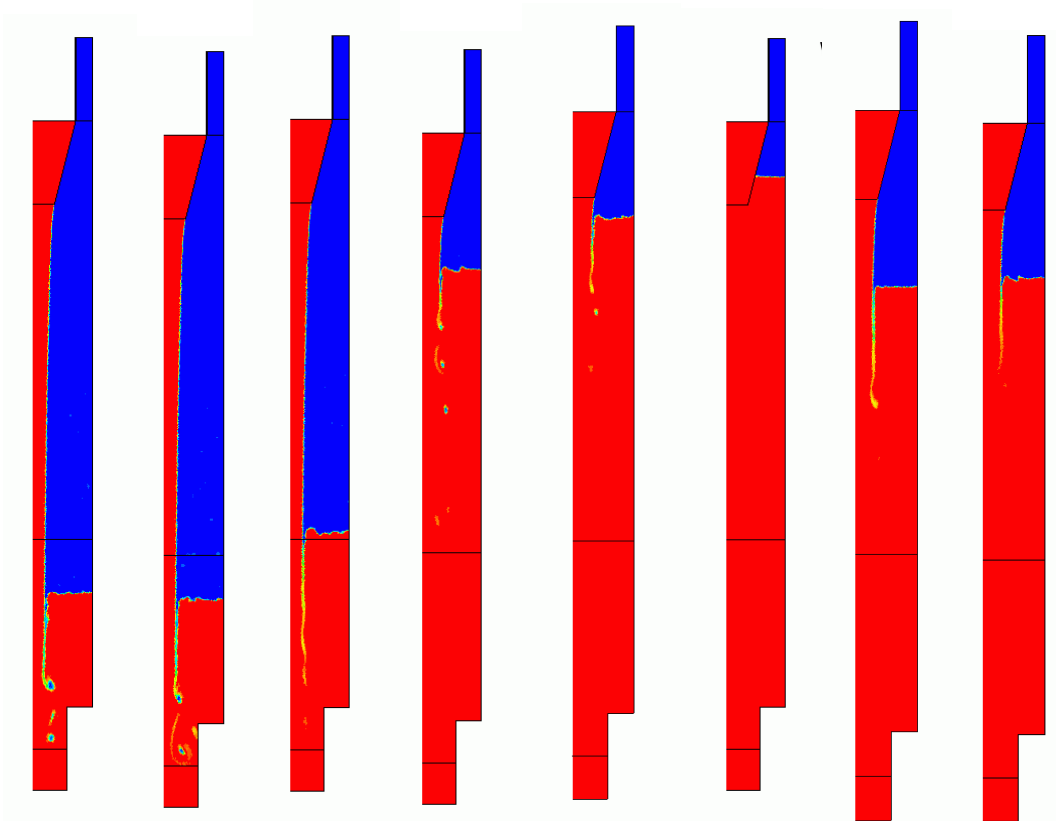


Figure 5: free fall second simulation. Volume fraction at times (s): 3, 5, 7, 12, 12.2, 16, 18, 20.

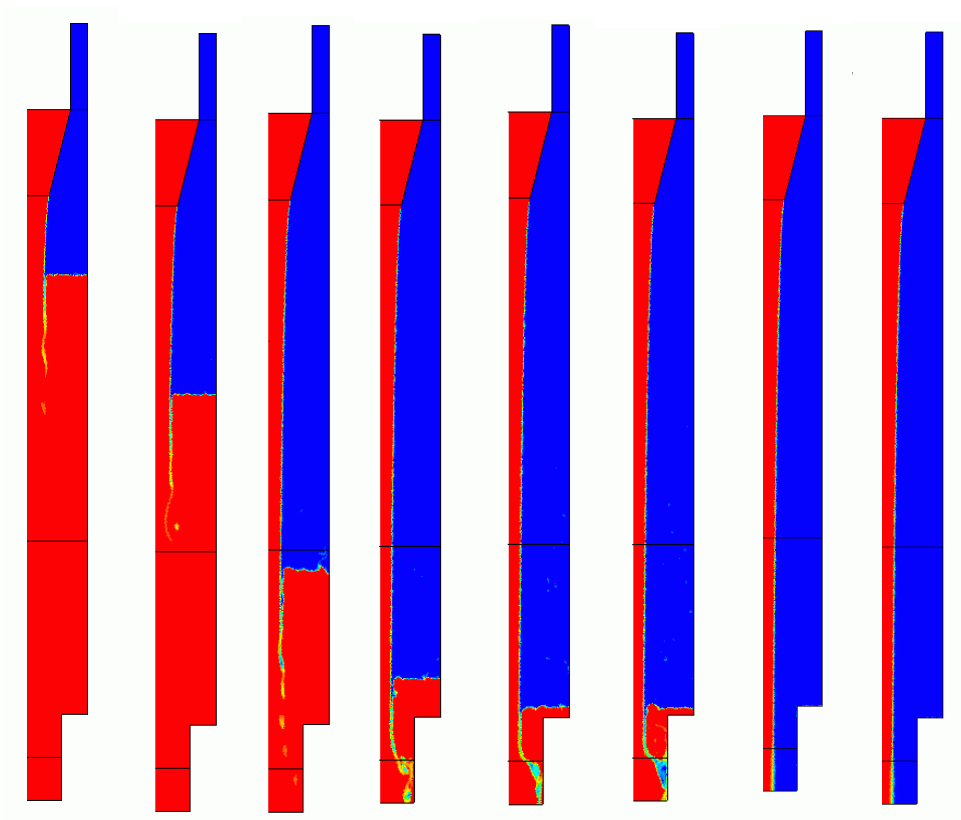


Figure 6: free fall second simulation. Volume fraction at times (s): 21-23-25-26-27-28-29-31.

## 5 Conclusion

Free fall without re-attachment can be perfectly handled with the Starccm+ VOF algorithm. In presence of shear stress, the condensation algorithm performs very well and allow to pursue simulations for large times keeping sense. The re-attachment to a stagnation region of a free falling jet is difficult to stabilize when small space is available. The re-attachment region seems to behave in any case under the given operating condition in a non stationary way. There are fundamental limitations with 2D or 2D+ simulations because the structure of the re-attachment region is believed to be both strongly un-stationary and fundamentally 3D.

## 6 References

[ 1] Carlucc, B., jardi, X., 2003. European project PDS XADS-preliminary design studies of an experimental accelerator driven system. In: Proc. Of the Int. Workshop on P&T and ADS Development, SCK-CEN,Mol,Belgium,p. A91

[2] <http://www.cd-adapco.com/>.

[3] Drag Limitation in the in the Three-Feeder Design, Katrien Van Tichelen SCK-CEN, 01-06-2007